JOURNAL OF APPLIED POLYMER SCIENCE VOL. 19, PP. 2319-2330 (1975)

Strain Energy Functions of Rubber. II. The Characterization of Filled Vulcanizates

A. G. JAMES* and A. GREEN, *Dunlop Research Centre, Kingsbury Road, Erdington, Birmingham, England*

Synopsis

In part I it was shown that if the strain energy function

$$W = \sum_{ij=0}^{\infty} C_{ij}(I_1 - 3)^i(I_2 - 3)^j$$

was expanded to a sufficient degree and the coefficients C_{ij} were found by regression to pure homogeneous strain data, then stress–strain equations could be derived to give accurate solutions to design problems even at relatively high extensions. The problems of applying this theory to filled vulcanizates are discussed and a way of obtaining pure homogeneous strain data for for such materials is suggested. Stress–strain equations fitted to the data are found to be general within the range of experimental strains and in some cases will extrapolate outside this range. The equations can be used in design applications where strains are greater than would be experienced in normal engineering practice.

INTRODUCTION

The purpose of the work described was to find a strain energy function sufficiently general for use in computer oriented iterative design methods. Within the limitations of a strain energy function, these techniques are capable of solving problems involving large deformations of complex shapes, where edges or folds may act as stress raisers giving regions of very high strain. Initially, the range of these local deformations in a particular problem is indeterminate, and a more comprehensive strain energy function increases the likelihood of obtaining an accurate result.

In part I, a way of presenting general homogeneous strain data was suggested and it was found that where stress–strain equations derived from elasticity theory were fitted to data to determine their coefficients, the resulting relationships could be used in design calculations even at strains outside the range of normal engineering practice. However, these principles were established using a gum vulcanizate, in which the stresses are independent of the order of application of the strains. The purpose of the work described in this part was to determine whether or not these ideas could be extended to cover vulcanizates containing inorganic fillers, which are of greater practical interest but whose characterization is complicated by stress history effect and whose stresses are affected by the order of application of the strains.

* To whom all communication should be addressed at: 17 Moor Meadow Road, Sutton Coldfield, Birmingham B 75 6 BU, West Midlands, England.

Stress-Softening

In any investigation involving the deformation of filled vulcanizates, care must be taken to allow for the effects of stress softening. To obtain the data of Figure 2 in part I for natural rubber (NR) gum, an arbitrary regime of softening of biaxial tensile test pieces was adopted; but the softening was found to have little effect on the data. In filled rubbers, the degree of softening is much greater, and there are other effects such as the long recovery time of these materials which makes this type of data more difficult to obtain. Some consideration has been given to these effects in order to ascertain the best method of obtaining pure homogeneous strain (PHS) data most relevant to engineering design.

The nature of stress softening in simple extension is well documented.[1-5] It is known that a test piece stretched for the first time in simple extension will be stiffer than on subsequent stretches to this extension. This softening continues for up to ten stretches before an equilibrium is reached, although most of the softening occurs during the first cycle. The softening is evident only to the level of extension of the previous prestretch.

Dannenberg[3] put the effect on a quantitative basis by showing that the amount of softening (defined as the decrease in work done on the test piece to reach a fixed deformation on subsequent stretches) depended on the work done on the test piece during the previous prestretch. Mullins[1] noted that if dumbbells were cut from a stretched sheet both in the direction of stress and perpendicular to this direction, then the softening appeared to be less in the perpendicular direction than in the direction of stress.

Another effect which has been noticed in stress-softened rubber is the effect on tear strength. Janssen[5] stretched rubber sheets and then measured the tear strength in the direction of prestretch and perpendicular to the direction of prestretch. After stretches greater than 250% extension, a permanent effect of reduced tear strength in the direction of prestretch and increased tear strength perpendicular to the direction of prestretch was observed. A structuring due to filler presence and crystallization was postulated to account for these effects which were not as evident in noncrystallizing rubbers.

In the stretching of an unsoftened biaxial tensile test piece, the following effect is observed. If a deformation of the test piece defined by the principal extension ratios λ_{A_1}, λ_{B_1} ($\lambda_{A_1} \neq \lambda_{B_1}$) caused by principal stresses σ_{A_1}, σ_{B_1} is immediately changed to λ_{A_2} ($= \lambda_{B_1}$), λ_{B_2} ($= \lambda_{A_1}$), the new stresses σ_{A_2}, σ_{B_2} are not equal to σ_{A_1}, σ_{B_1}. Thus, in order to establish the stress softening procedure, which would yield the most useful experimental result, some investigation of stress softening in deformations other than simple extension was carried out.

Stress Softening in General Deformation

Figure 1 is a typical graph showing the progressive softening of a filled vulcanizate deformed in simple extension. Only extension curves are shown. The numbers 1 to 5 refer to the 1st to 5th extension stress–strain curves. The test piece was stretched on an Instron tester first to A, then relaxed; then to B and relaxed; and so on. Figure 1 shows that the test piece is softened up to the maximum extension of the previous stretch and then follows what would be the stress–strain relationship of the virgin vulcanizate. This type of plot was suggested by Mullins and Tobin.[2] To demonstrate this effect, for example, to ob-

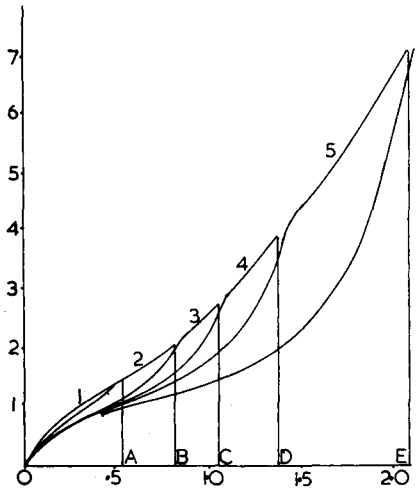

Fig. 1. Stress softening in simple extension. Abscissa: strain; ordinate: stress (MN/m²).

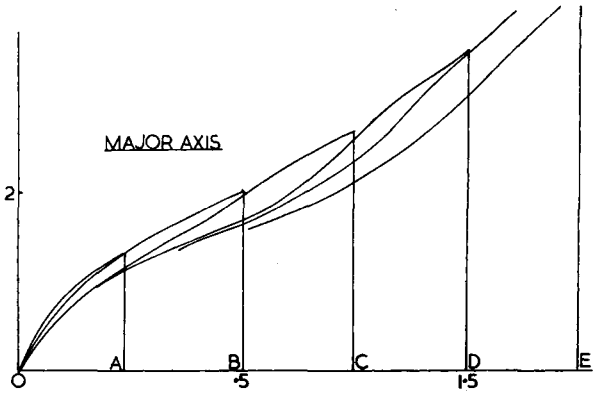

Fig. 2. Stress softening in pure shear. Abscissa: strain; ordinate: stress (MN/m²).

tain the experimental data for Figure 1, care must be taken to allow sufficient recovery time between successive stretches and to redraw the strain datum at the end of each recovery period. If insufficient recovery time is allowed (i.e., not long compared with the experimental time), apparent hardening of the material is observed at elongations higher than the previous extension. This was thought to be the result of regridding a test piece which is still recovering, giving an incorrect gauge for the next extension.

The biaxial tensile tester was used to obtain diagrams analogous to Figure 1 in pure shear ($\lambda_1 = \lambda$, $\lambda_2 = 1.0$, $\lambda_3 = 1/\lambda$) and equibiaxial extension ($\lambda_1 = \lambda_2$ and $\lambda_3 = 1/\lambda_1^2$). The material used in this investigation was an NR compound with 50 pphp HAF black. The test pieces were stretched and then relaxed for at least half an hour before regridding and further stretching to some higher extension.

Figures 2 and 3 illustrate the data obtained in pure shear; the former shows the stresses in the direction of extension, and the latter, the stress in the direction of the constant extension ratio $\lambda = 1.0$.

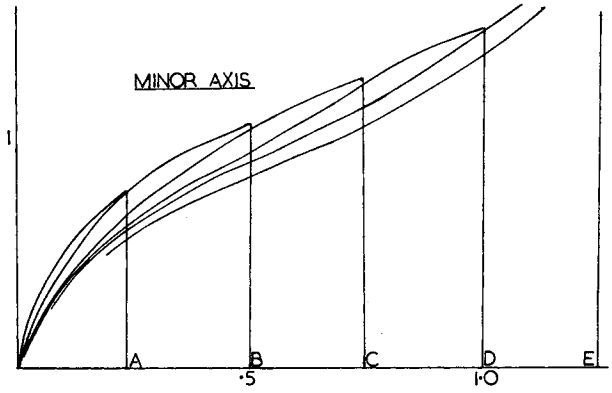

Fig. 3. Stress softening in pure shear. Abscissa: strain; ordinate: stress (MN/m²).

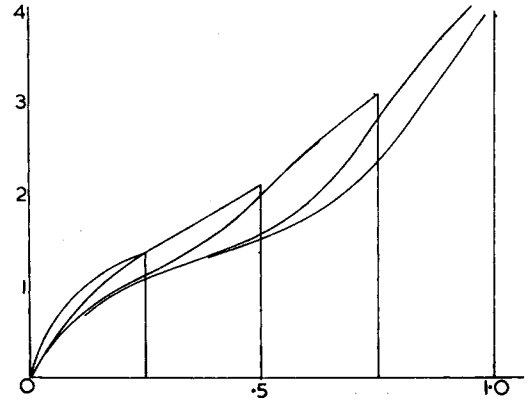

Fig. 4. Stress softening in equibiaxial extension. Abscissa: strain; ordinate: stress (MN/m²).

Figure 4 shows the result of subsequent extensions in equibiaxial extension (equibiaxial extensions are equivalent to unidirectional compressions).

All three figures show substantially the same picture for shear and compression as was seen to occur in simple extension. In order to be more quantitative about these similarities, test pieces were extended to approximately the same work input in tension, shear, and compression. The degree of softening was taken as the ratio of the energy input for the second cycle to the energy input for the first cycle.

The results can be summarized as shown in Table I. Although it was difficult to choose identical work inputs, it is evident that the degree of softening is about the same in each case. To a first approximation, we can make the general

TABLE I

Type of deformation	Energy input, MN/m²	Per cent softening, %
Simple extension	13.8	16
Pure shear	13.8	17
Equibiaxial extension	15.9	14

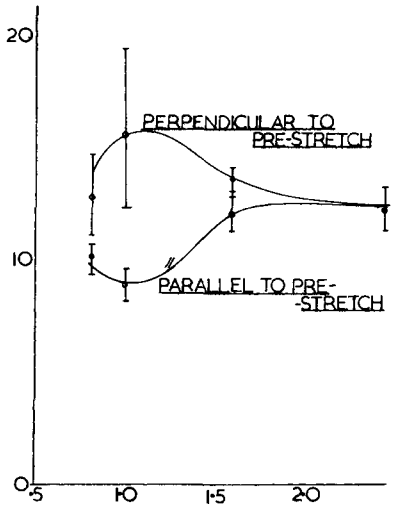

Fig. 5. Tear strength at $\lambda_1 = 2.4$ for four values of λ_2. Abscissa: extension ratio λ_2; ordinate: stress (MN/m^2).

point that stress softening is qualitatively and quantitatively independent of the type of deformation.

According to Mullins,[1] some softening occurs in the direction perpendicular to the direction of prestretch in a simple extension experiment. Figure 3 shows the same effect in pure shear. Mullins thought that the softening was less in the perpendicular direction than in the direction of prestretch. Thus, a test piece which has been softened in tension or shear would no longer be isotropic.

Another way of demonstrating the residual anisotropy resulting if a test piece is not uniformly softened is seen in the results of tear tests carried out on "delft" tear test pieces cut perpendicular and parallel to the direction of prestretch. This was investigated for test pieces which had been extended in simple extension, shear, and compression and in a deformation intermediate to shear and compression defined by $\lambda_1 = \lambda$, $\lambda_2 = 1.7$, $\lambda_3 = 1/1.7$. The maximum values of λ_1 in each experiment was $\lambda = 2.4$.

In Figure 5, the tear strengths parallel and perpendicular to the direction of largest prestretch are plotted as a function of the strain perpendicular to this direction. A definite residual anisotropy is evident where the test piece has been prestretched unequally in two directions.

The PHS Plot for Filled Vulcanizates

The purpose of stress softening is to achieve properties which will be unaltered during further deformations. In the stress softening investigations described here, changes in properties were confined to the first ten deformations. A biaxial tensile test piece made from a filled vulcanizate, softened by ten equibiaxial extensions in the two principal directions, became stable and isotropic in these directions. The effect on properties in the third direction is not yet known although the equibiaxial extension is equivalent to a uniaxial compression in the third direction with the same energy of deformation. Therefore it may be that the test piece has achieved three-dimensional stability. Experiments are being considered to investigate this proposition.

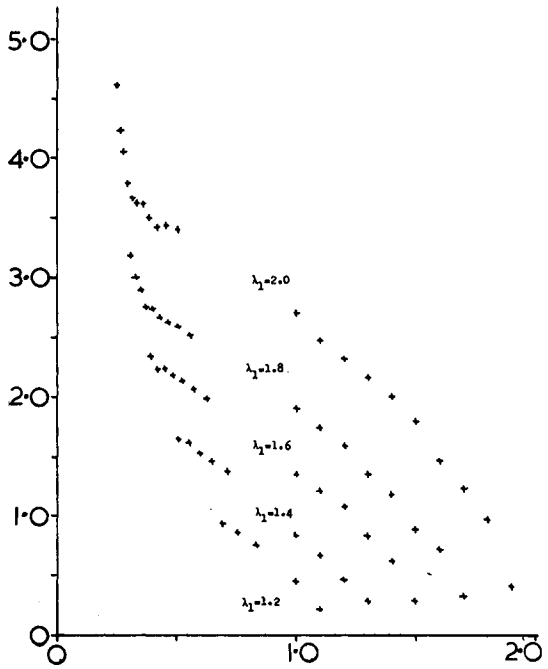

Fig. 6. PHS plot NR + 40 HAF. Abscissa: extension ratio (λ_2), ordinate: $\sigma_1 - \sigma_2$ (MN/m^2).

Consideration has been given to softening a biaxial test piece in the way most relevant to the intended use of the derived general stress–strain equation. To obtain a PHS plot such as Figure 2, part I, for a filled vulcanizate, a procedure was developed which incorporates the following conclusions:

a. The material must be softened to a stable state, otherwise successive measurements are made on a material with changing properties.

b. The material will be softened by an unrealistically large amount by precycling to deformations larger than the experimental range. Therefore, progressive softening as testing proceeds from the low deformations upward is suggested.

c. Because of the low recovery rate of the filled materials, it is suggested that between measurements, a recovery time which is large compared with the measurement time is allowed.

d. Strain data should be remarked between successive measurements to compensate for any permanent set effects.

e. Quasi-equilibrium stress–strain equations are being determined, and therefore a realistic relaxation time must be allowed at each measurement position.

f. Finally, if the test piece is extended to some deformation λ_{A_1}, λ_{B_1}, where these are the principal extension ratios, and if the stresses σ_{A_1}, σ_{B_1}, acting perpendicularly to each other, cause these deformations, then even with the precautions listed above, reversing the stress values (i.e., making $\sigma_{A_2} = \sigma_{B_1}$ and $\sigma_{B_2} = \sigma_{A_1}$) will not exactly reverse the deformations. This is possibly because of the sort of structuring effect suggested by Jansen.[5] To compensate for this, a technique has been incorporated into the testing procedure whereby values are reversed as described above and any differences are averaged.

TABLE II[a]

Compound	A	B	C	D
Natural rubber	100.00	100.00	100.00	100.00
Sulfur	2.50	2.50	2.50	2.50
C.B.S.	0.50	0.50	0.50	0.50
Stearic acid	2.00	2.00	2.00	2.00
ZnO	5.00	5.00	5.00	5.00
Mineral oil	5.00	5.00	5.00	5.00
Nonox ZA	0.15	0.15	0.15	0.15
Nonox BLB	1.70	1.70	1.70	1.70
HAF	40.00	50.00	60.00	70.00

[a] Cure 15–50 at 135°C.

TABLE III
Filler Effects

	Residual deviation, MN/m^2				
Approximation	NR Gum	NR + 40	NR + 50	NR + 60	NR + 70
Mooney	0.087	0.14	0.4	1.1	1.8
3rd-Order invariant	0.051	0.076	0.09	0.17	0.24
3rd-Order deformation	0.055	0.076	0.10	0.22	0.40
4th-Order deformation	0.040	0.076	0.10	0.22	0.30

The testing procedure was used to obtain the PHS plot (Fig. 6) for a filled natural-rubber vulcanizate. The experimental data are tabulated in Appendix II. It has been found that by limiting the experimental extensions in the range $\lambda_1 = \lambda_2 = 1.0 \rightarrow 2.0$, the data obtained exhibit very little scatter, as shown. With many filled polymers, tear strength prohibits testing at higher deformations; but in any case, the range chosen includes more severe deformations than those which a filled vulcanizate is subjected to in practice. Moreover, when the coefficients of a general stress–strain equation are found by regression to these data, the equation will often extrapolate to strains outside this experimental range.

PHS plots were obtained according to the method described above for a range of filled materials. The compounding details are given in Table II. The materials were natural-rubber vulcanizates compounded with different levels of an HAF filler, giving test pieces with a range of stiffnesses. The data obtained were analyzed according to the Mooney equation, the third-order invariant approximation, and the third- and fourth-order deformation approximation. In Table III, the residual deviations of the data about each regression are shown. In general, if the residual deviations for a particular material are compared, better fits are obtained when higher-order terms are included. In Tables A1, A2, A3, and A4 of Appendix I are the elastic constants (regression coefficients) for the range of materials relevant to the four forms of strain energy approximation. These equations have been used to predict practical results such as the simple extension stress–strain curve and the shape and pressure of inflated diaphragms. They were found to be accurate within the strain range covered by the PHS plot, and the lower the residual deviation to this plot, the more accurate the practical prediction.

Inflated Tube Profiles

In part I, it was shown that iterative techniques could be used to predict the shape of a tube which was inflated to pressure P, the ends of the tube being free to find their own position. The profiles of tubes made from the compound (NR/50HAF) were measured experimentally. The shape taken up by the tubes is sensitive to the addition of a reinforcing filler, and this experiment is therefore a useful tool for comparing stress–strain equations of a filled rubber.

It was found that the stress–strain equations derived from the nine-constant third-order invariant expansion of the strain energy function could only be used to predict tube profiles if the greatest strains in the tube surface were less than the greatest strains involved in the PHS plot. The five-constant and eight-

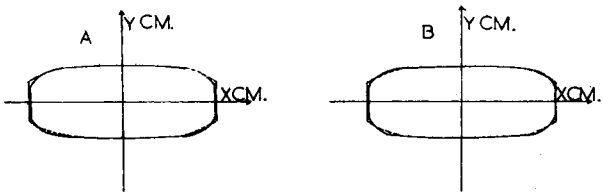

Fig. 7. Tube profiles at maximum circumferential strain $\lambda = 2.42$: (A) Third-order deformation approximation—experimental profile; (B) fourth-order deformation approximation—theoretical profile.

constant third- and fourth-order deformation expansions, however, predicted tube profiles outside this range, and in Figure 7, these predictions for a maximum circumferential strain of $\lambda = 2.42$ are compared with experimental results. The agreement is seen to be excellent.

The Calculation of Young's Modulus

Sets of constants have been given which each relate to the elastic nature of a particular vulcanizate. However, the compounder or technologist may justifiably point out that these are merely regression coefficients and request some means of relating them to quantities which are within his experience and which will enable him to identify the compound type. Consideration of the following points may be helpful.

The general stress–strain equation is of the form

$$\sigma_1 - \sigma_2 = 2(\lambda_1^2 - \lambda_2^2)\left|\frac{\partial W}{\partial I_1} + \lambda_3^2 \frac{\partial W}{\partial I_2}\right|$$

for simple extension; and with some approximation of the strain energy function, this becomes

$$f = 2(\lambda - 1/\lambda^2)\left|(C_{10} + C_{11}(I_2 - 3) + 2C_{20}(I_1 - 3) - - - - + \right.$$
$$\left. 1/\lambda^4(C_{01} + C_{11}(I_1 - 3) + 2C_{02}(I_2 - 3) - - - -)\right| \ldots \quad (5)$$

where f is the stress referred to the original cross section.

Young's modulus E is defined as

$$E = \left|\frac{df}{d\lambda}\right|_{\lambda \to 1}$$

If eq. (5) is differentiated with respect to λ, and λ tends to unity, we find

$$\left|\frac{df}{d\lambda}\right|_{\lambda \to 1} = E = 6C_{10} + 6C_{01}.$$

Terms involving constants other than C_{10} and C_{01} disappear. Thus, for any system of logical approximation of the strain energy function, Young's modulus E will be given by 6 times the sum of the constants C_{10} and C_{01}.

For the materials discussed in this paper and for the different types of approximation, $6(C_{10} + C_{01})$ has been calculated. The results are tabulated in Table IV. In parentheses next to the name of the vulcanizate, values of E_1 as measured on a Dynamic Response Apparatus[6] at 20% strain and 1.5 Hz are also included. It may be observed that the values of E calculated from $6(C_{10} + C_{01})$

TABLE IV

Material	$6(C_{10} + C_{01})$ Values, MN/m²			
	Mooney	5-Term	8-Term	9-Term
NR Gum (1.90)	1.32	1.41	1.50	1.33
NR + 40 (4.42)	3.03	3.07	3.20	3.13
NR + 50 (5.08)	4.13	4.28	4.30	4.33
NR + 60 (6.16)	6.49	6.56	6.29	6.27
NR + 60 (7.72)	9.37	6.47	9.20	8.16

are in good agreement for each type of approximation, except perhaps at the highest filler loading. Also, they are similar to those measured dynamically, although some variation would be expected owing to the effects of frequency and the more severe softening of the biaxial test pieces.

CONCLUSIONS

An experimental method has been developed to determine the values of the coefficients in any general stress–strain equation which can be arranged in a form suitable for multiple linear regression. It has been shown that with certain precautions, the technique can be applied to practical filled vulcanizates, and any deviation of these materials from the assumption of incompressibility has no significant effect on the pure homogeneous strain diagram upon which the experiment is based. A better representation of these quasi-equilibrium data is obtained where higher-order terms of the expansion of

$$W = \sum_{ij=0}^{\infty} C_{ij}(I_1 - 3)^i(I_2 - 3)^j$$

are included. A third-order deformation approximation of the strain energy function can be used to derive general relationships between stress and strain, which are independent of the material under consideration, are accurate enough for most practical engineering design purposes, and take the form

$$\sigma_i - \sigma_j = 2(\lambda_i^2 - \lambda_j^2)\left|\frac{\partial W}{\partial I_1} + \lambda_k^2 \frac{\partial W}{\partial I_2}\right|$$

where

$$\frac{\partial W}{\partial I_1} = C_{10} + 2C_{20}(I_1 - 3) + 3C_{30}(I_1 - 3)^2 + C_{11}(I_2 - 3)$$

and

$$\frac{\partial W}{\partial I_2} = C_{01} + C_{11}(I_1 - 3).$$

They, therefore, contain five of the coefficients C_{ij} which are constant for a particular material but will presumably be dependent upon temperature. Almost without exception, a sign convention was observed whereby C_{10}, C_{01}, and C_{30} were found to be positive and C_{11} and C_{20} negative.

Appendix I

TABLE A1

Material	Mooney constants, MN/m²	
	$C_{10} \times 10^{-1}$	$C_{01} \times 10^{-2}$
NR Gum	2.12	0.79
NR + 40	4.73	3.22
NR + 50	6.20	6.91
NR + 60	9.21	16.04
NR + 70	13.10	25.19

TABLE A2

Material	3rd-Order invariant approximation constants, MN/m²								
	C_{10}	C_{01}	C_{11}	C_{20}	C_{02}	C_{21}	C_{12}	C_{30}	C_{03}
NR Gum	2.11×10^{-1}	2.15×10^{-2}	-1.78×10^{-3}	-8.25×10^{-4}	10.5×10^{-5}	8.23×10^{-5}	-1.45×10^{-5}	7.16×10^{-5}	7.10×10^{-7}
NR + 40	4.9×10^{-1}	3.1×10^{-2}	1.29×10^{-3}	27.9×10^{-3}	1.9×10^{-3}	-7.71×10^{-3}	3.22×10^{-3}	12.7×10^{-3}	-4.6×10^{-4}
NY + 50	6.9×10^{-1}	3.2×10^{-2}	10.6×10^{-2}	-16.1×10^{-2}	-3.2×10^{-2}	-7.2×10^{-2}	2.9×10^{-2}	7.1×10^{-2}	-3.6×10^{-3}
NR + 60	8.3×10^{-1}	21.5×10^{-2}	-2.0×10^{-2}	-8.7×10^{-2}	-3.0×10^{-2}	-8.1×10^{-2}	4.4×10^{-2}	9.0×10^{-2}	-6.8×10^{-3}
NR + 70	10.25×10^{-1}	19.4×10^{-2}	-1.7×10^{-2}	-3.1×10^{-2}	3.3×10^{-2}	-5.5×10^{-2}	2.5×10^{-2}	11.6×10^{-2}	-4.8×10^{-3}

TABLE A3

Material	3rd-Order deformation approximation constants, MN/m²				
	C_{10}	C_{01}	C_{20}	C_{11}	C_{30}
NR gum	2.17×10^{-1}	1.76×10^{-2}	-2.41×10^{-3}	-6.4×10^{-4}	16.8×10^{-5}
NR + 40	4.7×10^{-1}	4.1×10^{-2}	-1.1×10^{-2}	-1.1×10^{-2}	6.4×10^{-3}
NR + 50	6.3×10^{-1}	8.4×10^{-2}	-4.1×10^{-2}	-3.3×10^{-2}	2.1×10^{-2}
NR + 60	8.9×10^{-1}	20.4×10^{-2}	-8.9×10^{-2}	-9.2×10^{-2}	5.4×10^{-2}
NR + 70	8.5×10^{-1}	22.9×10^{-2}	-11.4×10^{-2}	5.2×10^{-2}	5.7×10^{-2}

TABLE A4

Material	4th-Order deformation approximation constants, MN/m²							
	C_{10}	C_{01}	C_{20}	C_{11}	C_{30}	C_{21}	C_{02}	C_{40}
NR Gum	2.2×10^{-1}	2.92×10^{-2}	-5.7×10^{-3}	-2.8×10^{-4}	7.8×10^{-4}	1.2×10^{-4}	-4.7×10^{-5}	-3.0×10^{-5}
NR + 40	4.9×10^{-1}	4.3×10^{-2}	-2.2×10^{-2}	-1.5×10^{-2}	1.1×10^{-3}	1.0×10^{-3}	-2.3×10^{-5}	-6.7×10^{-4}
NR + 50	6.2×10^{-1}	9.7×10^{-2}	-3.1×10^{-2}	-4.4×10^{-2}	2.1×10^{-2}	2.4×10^{-2}	18.0×10^{-4}	-9.9×10^{-5}
NR + 60	9.9×10^{-1}	5.9×10^{-2}	-1.24×10^{-3}	-1.76×10^{-2}	4.2×10^{-2}	-3.1×10^{-2}	1.4×10^{-2}	8.6×10^{-3}
NR + 70	11.5×10^{-1}	21.0×10^{-2}	-1.7×10^{-1}	-1.8×10^{-1}	1.4×10^{-2}	-1.2×10^{-2}	3.1×10^{-2}	-6.0×10^{-3}

Appendix II

PHS Plot Experimental Data—Natural Rubber + 40 HAF

(See Fig. 6)

Extension ratio λ_1	Extension ratio λ_2	Engineering stress F_1/A_0, MN/m²	Engineering stress F_2/A_0, MN/m²
1.2	1.0	0.633	0.299
1.2	1.1	0.720	0.580
1.2	1.2	0.787	0.773
1.4	1.0	0.985	0.541
1.4	1.1	1.043	0.720
1.4	1.2	1.092	0.884
1.4	1.3	1.154	1.019
1.4	1.4	1.179	1.183
1.6	1.0	1.241	0.628
1.6	1.1	1.290	0.773
1.6	1.2	1.333	0.879
1.6	1.3	1.362	1.034
1.6	1.4	1.390	1.146
1.6	1.5	1.402	1.300
1.6	1.6	1.468	1.502
1.8	1.0	1.401	0.618
1.8	1.1	1.439	0.773
1.8	1.2	1.459	0.865
1.8	1.3	1.483	1.005
1.8	1.4	1.521	1.106
1.8	1.5	1.536	1.246
1.8	1.6	1.613	1.362
1.8	1.7	1.671	1.575
1.8	1.8	1.777	1.792
2.0	1.0	1.695	0.671
2.0	1.1	1.710	0.680
2.0	1.2	1.719	0.913
2.0	1.3	1.753	1.029
2.0	1.4	1.811	1.154
2.0	1.5	1.816	1.217
2.0	1.6	1.835	1.372
2.0	1.7	1.898	1.502
2.0	1.8	2.029	1.710
2.0	1.9	2.116	2.009
2.0	2.0	2.309	2.227

The authors wish to thank P. S. Oubridge and G. D. Hubbard for helpful criticism and discussion, and the Dunlop Co. for permission to publish this paper.

References

1. L. Mullins, *J. Rubber Res.*, **16**, 12 (1947).
2. L. Mullins and R. Tobin, *Proc. 3rd Rubber Tech. Conf., xx*, 1954, p. 397.
3. E. M. Dannenberg, *Cabot Research Paper*, 2–26 (1965).
4. J. A. C. Harwood and A. R. Payne, *J. Appl. Polym. Sci.*, **10**, 2 (1966).
5. H. J. J. Janssen, *Proc. 3rd Rubber Tech. Conf.*, 1954, p. 351.
6. J. Smith and C. Sumner, *Int. Rubber Conf.* Brighton, May 1972.

Received September 10, 1974
Revised December 23, 1974